Lasers in Engg., Vol. 14, pp. 133-151
Reprints available directly from the publisher
Photocopying permitted by license only

Studies On Residual Stress Developed In Laser Surface Irradiated 0.6% Carbon Steel

J. DUTTA MAJUMDAR[1*], A. K. NATH[2], B. RAVI KUMAR[3] AND I. MANNA[1]

[1] *Dept. of Met. & Mat. Engg., Indian Institute of Technology, Kharagpur – 721302, India*
[2] *Laser R & D Block-B, Centre for advanced Technology, Indore – 452013, India*
[3] *MST Division, National Metallurgical Laboratory, Jamshedpur*

Laser surface hardening is a process of microstructural modification of the near surface region of iron-based component by inducing martensitic transformation with a high power laser beam as a source of heat. The process is aimed at introducing a hard and wear-resistant layer on the surface, thereby increasing the service life of the component. Due to a rapid rate of heating and cooling and a large thermal gradient associated with the process, a measurable amount of residual stress is developed in the laser irradiated region. In the present investigation, an attempt has been made to surface harden medium carbon steel (0.6% Carbon) using 2.5 kW continuous wave CO_2 laser as a source of heat using Ar as shrouding gas. The microstructure and phase analysis of the irradiated region have been carried out in details. Residual stress developed in the laser-irradiated region has been carefully measured. Effect of laser parameters on microhardness and wear resistance has been studied. Finally, the processing zone for the surface hardening has been derived following a detailed structure-property correlation.

Keywords: *laser, hardening, steel, microhardness, wear, residual stress*

*Corresponding author: FAX: +91 3222 282280, e-mail: jyotsna@metal.iitkgp.ernet.in

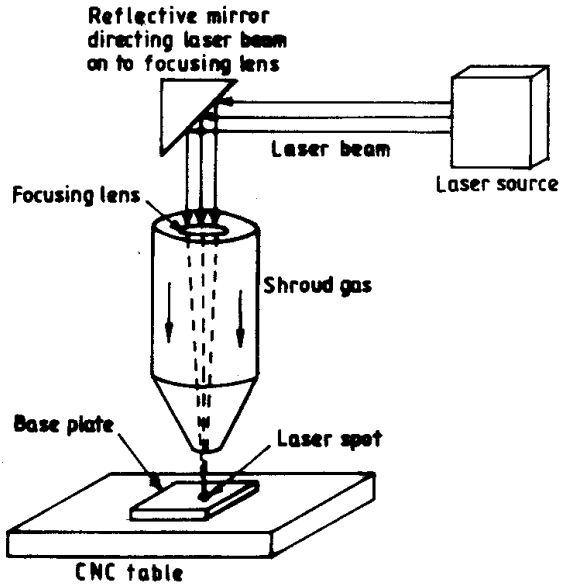

FIGURE 1
Schematic of experimental set-up of laser surface hardening.

INTRODUCTION

Surface microstructure and composition play a crucial role in determining important mechanical property such as wear resistance [1]. Flame and induction hardening are conventional techniques to improve the wear resistance of Fe-based substrate by inducing martensitic transformation on the surface. A larger heat affected zone and difficulty in process control are the most commonly encountered problems associated with the process. On the other hand, a high power directed laser beam may be used as a source of heat for surface hardening of Fe- based substrates known as laser surface hardening[2]. It is a well known process used to harden the near surface region of turbine blades, crank shafts and tractor engine components [3-5]. The process is characterized by a large thermal gradient of $10^5 - 10^8$ K/m and cooling rate of $10^4 - 10^{11}$ K/s [6-8]. Economy in time/energy consumption, precise control over the depth of hardening, minimum heat affected zone, cleanliness and ability to apply the technology to finished and semi-finished products are some of the advantages of laser surface hardening over conventional surface hardening techniques [6]. However, it should be pointed

TABLE I
Details of the laser parameters employed for laser surface irradiation of medium carbon steel (0.6% C) and characteristics of the surface layer.

Sl. No.	Applied power (kW)	Scan Speed (m/min)	Depth of hardening (μm)	Phases present	Microstress (MPa)	Microhardness (VHN)
1	0.95	1.0	135	Ferrite, cementite, retained austenite, martensite	Nil	690
2		1.5	105	Ferrite, cementite, retained austenite, martensite	Nil	725
3		2.0	85	Ferrite, cementite	Nil	240
4	1.2	1.0	155	Ferrite, cementite, retained austenite, martensite	33	625
5		1.5	130	Ferrite, cementite, retained austenite, martensite	14	500
6		2.0	120	Ferrite, cementite	23	220
7	1.55	0.5	700	Ferrite, cementite, δ-Fe	0	210
8		1.0	545	Ferrite, cementite, δ-Fe	0	235
9		1.5	450	Ferrite, cementite, retained austenite, martensite	20	350
10		2.0	300	Ferrite, cementite, martensite	8	600

out that the laser processing variables, i.e. laser power, beam diameter, scan speed, focusing conditions, shielding gas environments and material chemistry play a significant role in determining the microstructure and hence, the properties of the hardened layer. Laser transformation hardening consists of three processing steps: a. heating the substrate to a temperature above AC1, b. homogenization and c. rapid self-quenching. Laser parameters play a crucial role in creating the desired microstructure on the surface. Furthermore, a high thermal stress is generated in the laser irradiated surface resulting from the high cooling rate and thermal gradient associated with the process [9]. The presence of surface residual stresses, if tensile, may be equal to the applied stress and hence, leads to premature failure of the component [10]. In

the present study, laser surface hardening of a 0.6 % steel was carried out using a continuous wave CO_2 laser. A detailed study of the microstructure and phase analysis of the laser surface hardened zone has been conducted and correlated with laser parameters. The residual stresses developed due to the laser surface hardening have been measured and correlated with laser parameters. The optimum laser processing window was determined by correlating laser parameters with the microstructure, microhardner and residual stresses in the hardened zone. Finally, the mechanical properties of the surface, *i.e.*, microhardness and wear resistance have been studied in details.

EXPERIMENTAL

Prior to laser surface hardening (LSH), 0.6 % C steel sample surface (of 15 mm x 15 mm surface area and 5 mm thickness) was sand blasted to remove the surface oxide layer and roughen the surface to increase the absorptivity. Laser surface hardening was carried out using a 2 kW continuous wave (CW) CO_2 laser with a beam diameter of 1 mm with Ar as shrouding gas to avoid oxidation. The specimens were mounted on a water chilled copper block placed on a CNC controlled stage which could be moved at speeds of 100 – 4000 mm/min. The focal point of the beam was 30 mm above the specimen surface. Figure 1 shows the schematic of experimental set-up for laser surface hardening. The process variables in the present study were laser power and scan speed. An adequate number of trials were conducted to correlate the process parameters with the microstructure and optimize the laser parameters (Table 1). A detailed investigation of the microstructural evolution in the alloyed zone was undertaken both on the laser irradiated surface and in the plane perpendicular to the lased surface and lasing direction. The specimens were carefully mounted and ground initially on coarse polishing cloths to remove the surface oxide layer and subsequently mechanically polished using 200, 300, 600 and 1200 grade emery papers. Final polishing was carried out in a rotating wheel with 1 µm diamond paste to obtain a scratch free flat surface. The polished specimens were etched using 5% Nital (alcohol:HNO_3 = 95:5). The etching time was 30-45 s. A detailed microstructural investigation was then carried out. A graduated ocular was used to measure the maximum depth/width of the hardened zone on the cross section and correlated with laser power and the interaction time (= beamdiameter/scan rate). A detailed investigation on the variation of hardened zone microstructure with laser

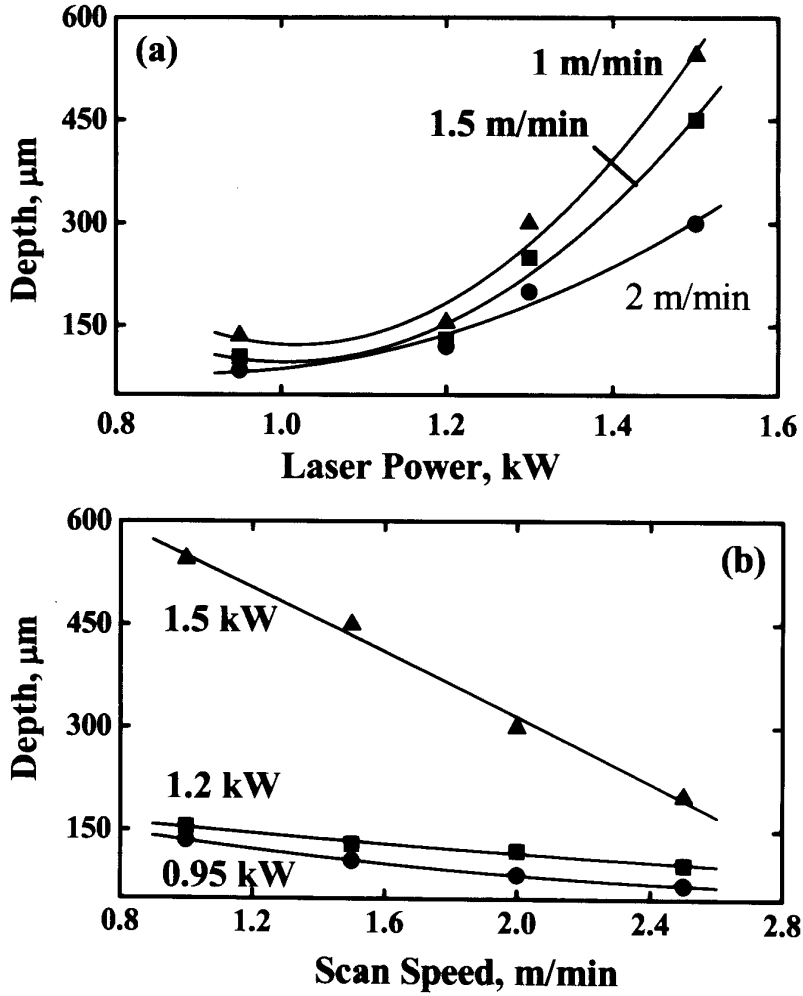

FIGURE 2
Variation of maximum depth of hardening of 0.6% C steel with (a) laser power and (b) scan speed.

barameters was undertaken using a CAMSCAN-2 scanning electron microscope (SEM). The phases formed were analyzed by X-ray diffractometer (XRD). The microhardness on the top surface and the cross-section of the laser surface hardened layer were measured by a Vickers microhardness tester with a 300 g applied load. The residual stresses developed during laser surface hardening were measured using X-ray

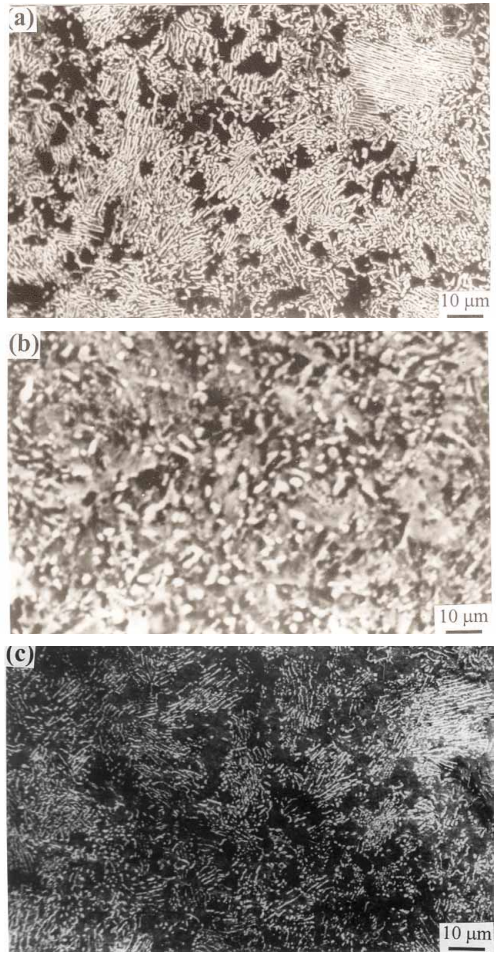

FIGURE 3
Scanning electron micrographs of the top surface of (a) as-received and laser surface hardened 0.6 % C steel lased with (b) a power of 0.95 kW, scan speed of 2 m/min; and (c) a power of 1.55 kW, scan speed of 0.5 m/min, respectively.

diffraction. Finally, the kinetics of wear of the as-received and laser surface hardened steel was measured by a Pin-on-Disc wear testing machine against a hardened steel disc under an applied load of 3 kg and 300 rpm wheel speed.

RESULTS AND DISCUSSION

Characteristics of the hardened zone

A detailed microstructural study of the hardened layer was conducted to correlate the laser processing parameters with the microstructure of the hardened layer. Selection of the laser parameters is critical to ensure complete austenitization and adequate quenching rate to form martensite. Apart from the microstructure, the depth of hardening also plays a role to determine the performance of any component. Hence, a systematic study of the effect of laser parameters on the depth of hardening was undertaken in the present study. Figures 2(a,b) show the dependence of the maximum depth of hardening for the 0.6% C steel with (a) laser power and (b) scan speed. In Figure 2(a) it can be seen that the depth of hardening increases with increase in laser power mainly because of increased depth of austenitization at a higher energy input. However, the application of a very high power causes melting of the surface and hence, should be avoided. On the other hand, application of a very low power may cause incomplete dissolution of carbides and hence, the formation of an inhomogeneous microstructure. An increase in scan speed, however reduces the interaction time and hence, the decreased energy input leading to decreased depth of austenitization (*cf*. Figure 2(b)). The microstructure of the hardened layer was found to vary with laser parameters. Laser irradiation of the surface layer causes heating and transformation of the surface layer to austenite, dissolution of carbides with subsequent quench-cooling. Application of inadequate power causes improper austenitization or a very high scan speed causes incomplete dissolution of carbides, due to insufficient time being available for the diffusion of carbon. On the other hand, the application of a very high power or very low scan speed may cause reduced a cooling rate and hence, reducing the volume fraction of martensite.

Figures 3(a-c) show scanning electron micrographs of the top surface of (a) as-received and laser surface hardened 0.6 % C steel lased at (b) a power of 0.95 kW, scan speed of 2 m/min; and (c) a power of 1.55 kW, scan speed of 0.5 m/min, respectively. The microstructure of the as-received steel consists of ferrite grains and pearlite colonies. The approximate volume fraction of pearlite was 75% as expected from the equilibrium phase diagram. Application of a very low power and a very high scan speed causes incomplete dissolution of carbide and partial transformation to austenite during heating. Rapid quenching leads to the presence of undissolved carbide, fine grained ferrite and very fine transformed pearlite which is unresolved (*cf*. Figure 3(b)). Application of a very high power and a low

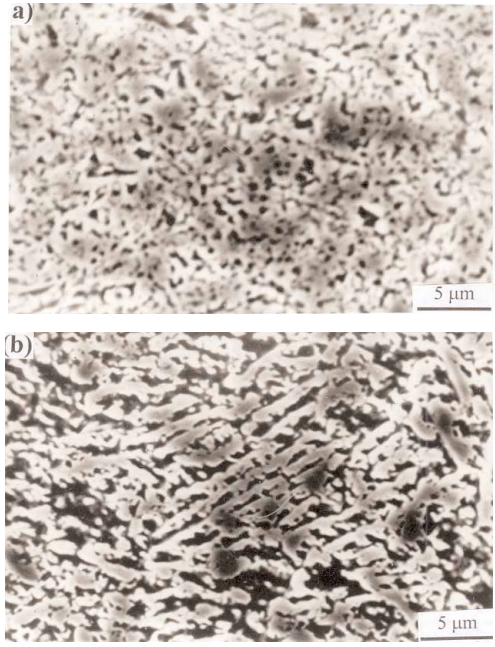

FIGURE 4
Scanning electron micrographs of the top surface of laser surface hardened 0.6 % C steel lased with a power of (a) 0.95 kW and (b) 1.2 kW (at a scan speed of 1 m/min).

scan speed causes melting of the substrate and rapid solidification leads to formation of austenite (untransformed) and fine pearlite due to the partial transformation of austenite (as shown in Figure 3(c) and subsequently, confirmed by XRD analysis). Hence, it is relevant from Figures 3(a-c) that improper selection of laser parameters is not conducive to the formation of a hardened layer. Figure 4(a,b) shows the microstructure of laser surface irradiated 0.6 % C steel lased at a power of (a) 0.95 kW and (b) 1.2 kW and at a scan speed of 1 m/min. Laser irradiation at 0.95 kW produces a combination of lath and acicular martensitic (*cf.* Figure 4a). Increasing the laser power causes formation of fine bainite (cf. Figure 4b). An increase in the applied power increases the temperature and changes the heat transfer such that there is isothermal holding in the bainitic region leading to the formation of bainite.

Figures 5(a,b) show the microstructure of the top surface of laser surface hardened 0.6% C steel lased at a power of 1.5 kW and scan speed of (a) 1 m/min and 1.2 m/min, respectively. Application of a high power and moderate

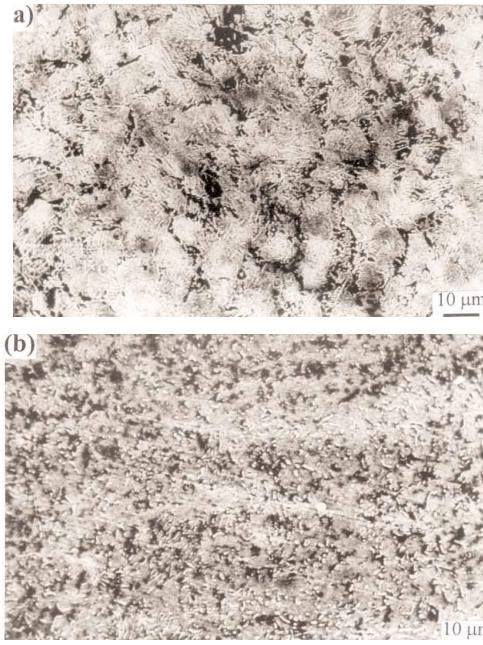

FIGURE 5
Scanning electron micrograph of the top surface of laser surface hardened 0.6% C steel lased with a power of 1.5 kW and scan speed of (a) 1 m/min and (b) 1.2 m/min, respectively.

scan speed leads to complete dissolution of carbide in austenite and the formation of a refined pearlitic colony (*cf.* Figure 5a). However, with an increase in the scan rate, the pearlite becomes finer (hence, unresolved) with the presence of very fine undissolved carbides (cf. Figure 5b).

A detailed X-ray diffraction study was conducted to identify and hence, confirm the phases present in the microstructure and to correlate it with the process parameters. Figures 6(a-c) show the X-ray diffraction profile of the top surface of (a) as-received and laser surface hardened 0.6 % C steel treated at (b) a power of 0.95 kW, scan speed of 2 m/min; and (c) a power of 1.55 kW, scan speed of 0.5 m/min, respectively. The X-ray diffraction profile of the as-received 0.6% C steel consists of mainly ferrite and a few carbide peaks. Application of inadequate power or interaction time does not change any phase distribution (as evident from Figure 6(b)), although the intensities of the Fe_3C phase increases, mainly because of the presence of undissolved carbide in the matrix. Application of very high laser pwer and very low scan speed leads to melting of surface. Subsequent solidification

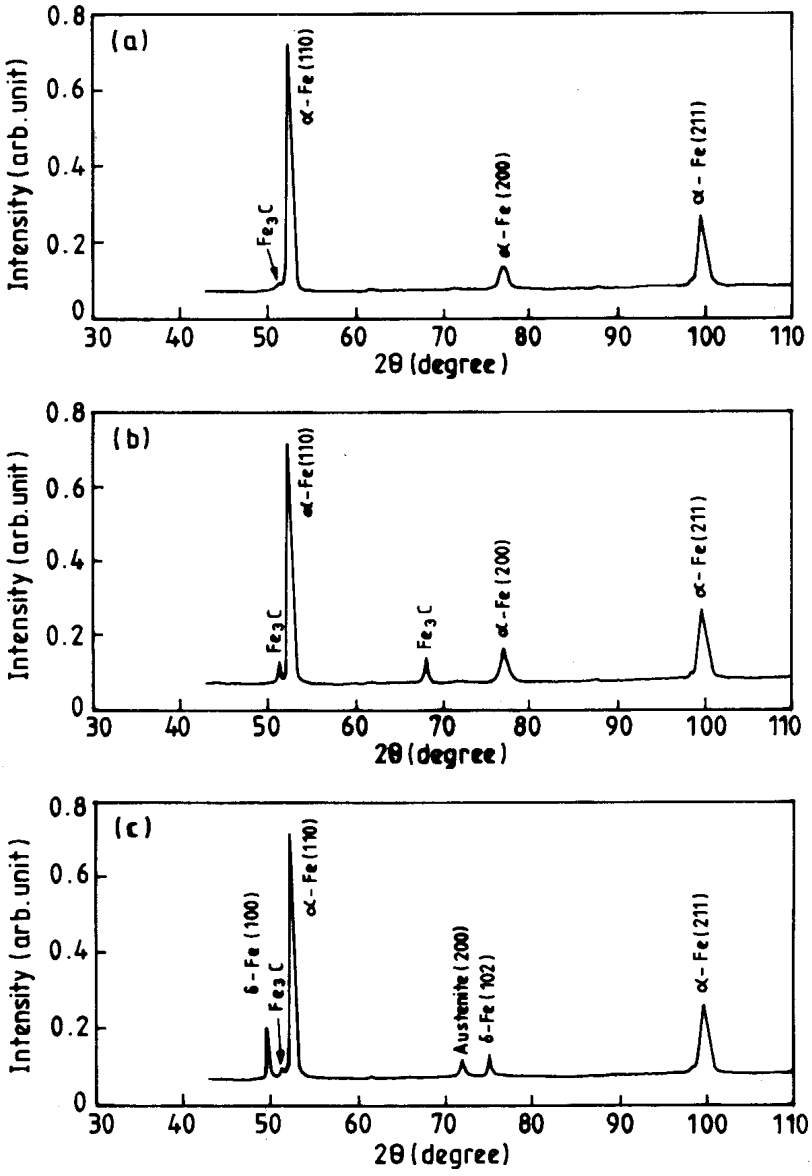

FIGURE 6
X-ray diffraction profile of the top surface of (a) as-received and laser surface hardened 0.6 % C steel lased with (b) a power of 0.95 kW, scan speed of 2 m/min; and (c) a power of 1.55 kW, scan speed of 0.5 m/min, respectively.

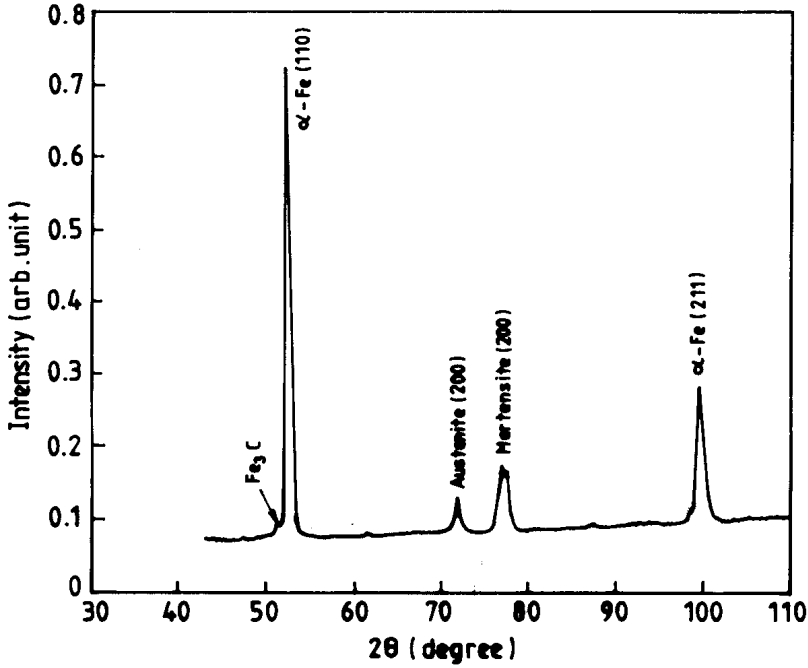

FIGURE 7
X-ray diffraction profile of laser surface hardened 0.6% C steel lased with a power of 0.95 kW and scan speed of 1 m/min.

leads to a presence of a few δ-ferrite and austenite peaks in addition to ferrite and Fe_3C peaks in the matrix (*cf.* Figure 6c). However, the presence of δ-ferrite was too small to be detected in the microstructure.

In contrast, an appropriate selection of the laser parameters leads to the formation of martensite with pearlite and retained austenite. Figure 7 shows the X-ray diffraction profile of the top surface of laser surface hardened 0.6% C steel lased at a power of 0.95 kW and a scan speed of 1 m/min. The presence of martensite in addition to retained austenite, ferrite and cementite peaks in the X-ray diffraction profile may be noted. Table 1 summarizes the results of the analysis derived from the X-ray diffraction study of laser surface hardened 0.6 % C steel as a function of laser parameters.

Residual Stress Developed on the Surface

Residual stresses developed during laser surface hardening were determined by X-ray diffraction . Both the macro and micro component of the stress have

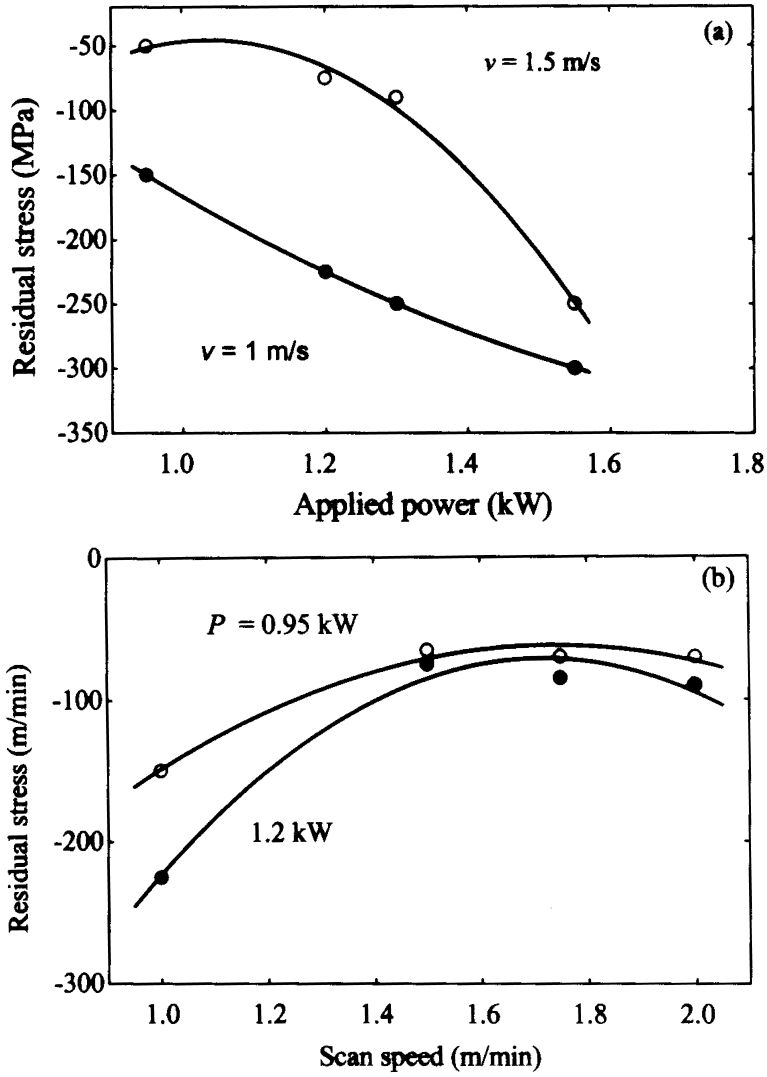

FIGURE 8
Residual stress developed in laser surface hardened 0.6 % C steel as a function of a) laser power and (b) scan speed.

been determined. A macro residual stress exists over a few grains and is measured from the displacement of the diffraction lines. On the other hand, micro residual stresses exists in a single grain and causes general broadening of

TABLE I
Details of the laser parameters employed for laser surface irradiation of medium carbon steel (0.6% C) and characteristics of the surface layer.

Sl. No.	Applied power (kW)	Scan Speed (m/min)	Depth of hardening (μm)	Phases present	Microstress (MPa)	Microhardness (VHN)
1	0.95	1.0	135	Ferrite, cementite, retained austenite, martensite	Nil	690
2		1.5	105	Ferrite, cementite, retained austenite, martensite	Nil	725
3		2.0	85	Ferrite, cementite	Nil	240
4	1.2	1.0	155	Ferrite, cementite, retained austenite, martensite	33	625
5		1.5	130	Ferrite, cementite, retained austenite, martensite	14	500
6		2.0	120	Ferrite, cementite	23	220
7	1.55	0.5	700	Ferrite, cementite, δ-Fe	0	210
8		1.0	545	Ferrite, cementite, δ-Fe	0	235
9		1.5	450	Ferrite, cementite, retained austenite, martensite	20	350
10		2.0	300	Ferrite, cementite, martensite	8	600

the diffraction line. Micro-residual stresses introduced during laser surface hardening was calculated from the line broadening of the high angle peak in the X-ray diffraction profile. On the other hand, the macro-residual stress was measured using a stress goniometer fitted to a Philips X-ray diffractometer. The micro-residual stress calculated from the peak broadening of an α-Fe(211) peak under various conditions of lasing are summarized in Table 1. Table 1 shows that the microstress developed on laser surface hardening could be varied from 5 to 35 MPa by changing the conditions. However, the variation in the microstress with laser power and scan speed was not found to follow any specific trend. Figures 8(a,b) summarize the residual macro-stress developed in laser irradiated 0.6 % C steel as a function of (a) laser power and (b) scan

TABLE II
Characteristics of the laser irradiated surface processed under different conditions as shown in the shaded region.

Position	Microhardness (VHN)	Phases Present
Zone I	350-750	Austenite, martensite, ferrite, cementite
Zone II	200-245	Ferrite and cementite
Zone III	200 — 235	δ-Ferrite, Austenite, ferrite, cementite

speed. The residual stress reported in Figure 8 is the average stress distribution over various regions on the surface of hardened layer. Figure 8a shows that the residual stress developed on the surface is predominantly compressive in nature (varying from –50 to –300 MPa) the magnitude of which increases with increasing laser power. The compressive nature of the residual stress is attributed to the transformation stress associated with the austenite to martensite transformation [9]. On the other hand, the magnitude of compressive residual stress is a maximum at a scan speed of 1 m/min, which significantly decreases with increase in scan speed (at 1.5 m/min) and remains almost constant thereafter. The decrease in the magnitude of the compressive residual stress with increase in scan speed is due to the incomplete dissolution of carbides in austenite due to the shorter interaction time and thus to the reduced transformation of austenite to martensite. From the macro- residual stress distribution it is evident that the present laser surface hardening routine introduces residual compressive stress on the surface which is beneficial in improving the fatigue life and wear resistance of the hardened component.

Microhardness of the hardened layer

Figure 9 shows the microhardness profiles of the laser surface hardened 0.6 % C steel (lased under some optimum processing conditions) as a function of the distance from the surface measured on the cross sectional plane of laser irradiated surface. The microhardness of the irradiated zone has increased significantly by 2 – 4 times (300 to 650 VHN) as compared to that of the substrate (180 VHN). The microhardness of the hardened zone is almost uniform throughout the cross section of the hardened layer and decreases gradually towards the interface of the melted zone. This improvement in microhardness due to laser surface hardening may be attributed partly to martensitic transformation and partly because of

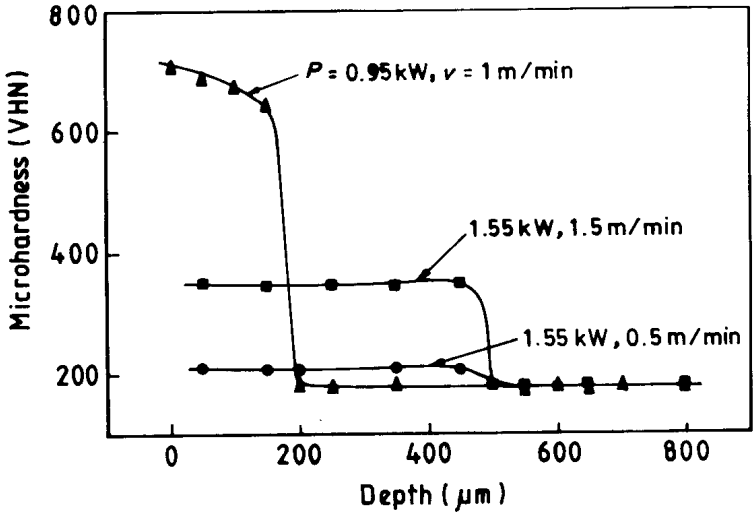

FIGURE 9
Microhardness profiles of the laser surface hardened 0.6 % C steel (processed under a few selected conditions as mentioned in Figure) as a function of vertical depth or distance from the surface measured on the cross sectional plane in the laser surface melted zone.

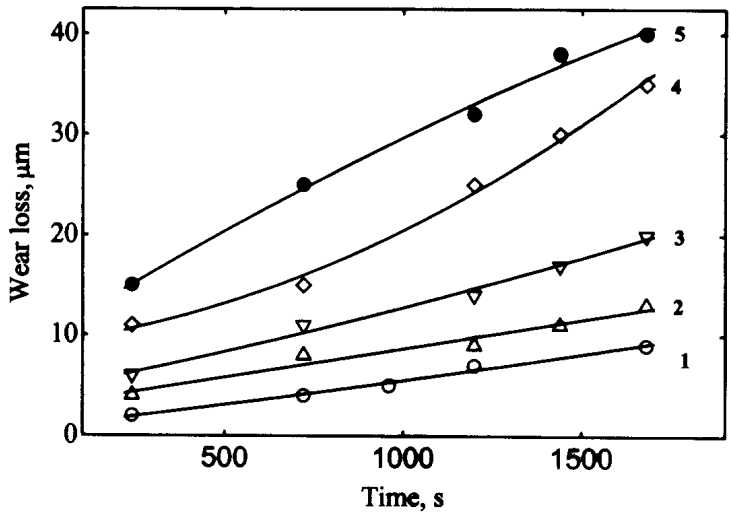

FIGURE 10
Kinetics of wear of the as-received (curve 5) and laser surface hardened steel lased with (1: power of 0.95 kW, scan speed of 1 m/min; 2: power of 0.95 kW, scan speed of 0.75 m/min; 3: power of 1.2 kW, scan speed of 1 m/min; 4: power of 1.55 kW, scan speed of 1 m/min) against hardened steel ball using 1 kg applied load.

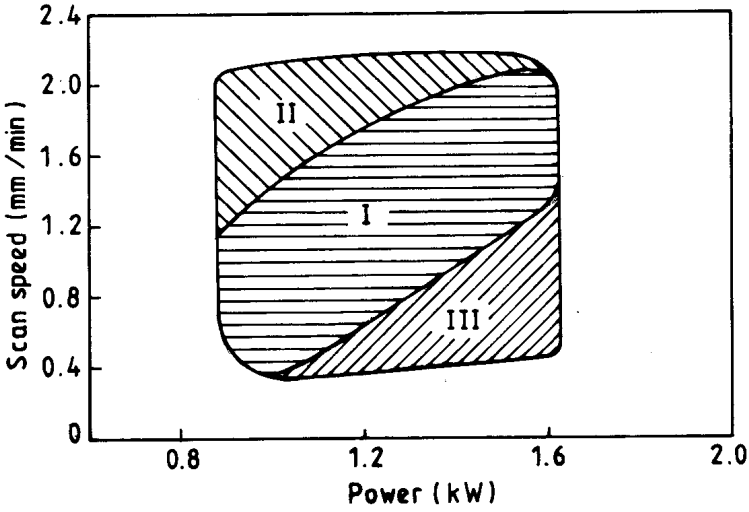

FIGURE 11
Optimum processing zone for laser transformation hardening of 0.6% C steel. The characteristics and properties of the shaded region are summarized in Table 2.

refinement of structure. Furthermore, the average microhardness in the laser surface hardened zone was found to vary with the laser parameters (laser power and scan speed). Figure 9 shows that the maximum microhardness is achieved at a power of 1.2 kW and a scan speed of 1 m/min. It may further be noted that lasing with a higher scan speed reduces the microhardness of the hardened zone significantly. The microhardness values achieved for different conditions of lasing are summarized in Table 1. Though micro hardness is not a direct measure of wear resistance, the significant enhancement in microhardness and refined microstructure produced by laser surface hardening may be effective in imparting a better resistance to wear in 0.6 % C steel components.

Evaluation of wear resistance

The wear loss of as-received and laser surface hardened steel (lased under different processing conditions) were measured by a Pin-on-Disc wear testing machine against a hardened steel disc with a 3 kg applied load and at 300 rpm wheel speed for a period between 1 min. to 3 h, and measuring the cumulative wear loss of materials at a regular intervals. Figure 10 compares the wear loss

of the as-received steel with those after various laser surface hardening treatments as a function of time. It may be noted that the wear loss is reduced by laser surface treatment. The wear behavior was however, dependent on the laser parameters used. The maximum wear resistance was achieved at a power of 0.95 kW and scan speed of 1 m/min. The microstructure of the laser surface irradiated steel at a power of 0.95 kW and scan speed of 1 m/min consists maimly of martensite, retained austenite, ferrite and cementite with a very high hardness (690 VHN) and hence, shows a superior abrasive wear resistance. Laser irradiation at a power of 1.55 kW and scan speed of 1 m/min causes melting occurs with formation of refined pearlite, ferrite and δ-iron resulting in marginally higher microhardness (235 VHN) than the as received material and as a result, the wear resistance is marginally higher than that of the substrate (curve 4 vis-à-vis curve 5). Consequently, it can be stated that the wear resistance is improved but the degree of improvement depends on the choice of the laser parameters and hence, the surface microstructure.

PROCESS OPTIMIZATION

Figure 11 shows the process parameter window for laser surface hardening of 0.6% C steel. The austenitizing temperature for a 0.6 % C steel is 750^0C [11]. Heating the substrate to a temperature below 750^0C will lead to incomplete austenitization and thus, the presence of ferrite in the microstructure. On the other hand, use of a very high scan rate results in incomplete dissolution of carbides (*cf*. Figure 3(b)). Transformation of austenite to martensite produces compressive residual stresses on the surface, which can improve the fatigue resistance. Furthermore, the microhardness of the modified layer is very dependent on microstructure. Accordingly, the processing zone in Figure 11 has been divided into three different isomicrostructure and property regions. There are three different iso-microstructure and property regions. The characteristics and properties of the shaded region in Figure 11 are summarized in Table II. The residual stress is mainly compressive although its magnitude is very small. Region II in Figure 11 defines the domain of incomplete dissolution of carbides and the presence of a higher volume fraction of carbides in the microstructure. Laser irradiation in region III causes melting of the surface and the residual stress changes to tensile, the microstructure is ferrite-pearlite with the presence of δ-iron and a very refined morphology. In region I a hardened layer is formed with the presence of higher volume fraction of martensite

and a significantly higher microhardness (600 – 775 VHN). Hence, laser parameters should be carefully chosen to induce a hardened zone with a high microhardness and wear resistance.

SUMMARY AND CONCLUSIONS

In the present investigation, laser surface irradiation of a medium carbon steel (0.6 % carbon steel) was carried out with a continuous wave CO_2 laser at a power ranging from 0.95 to 1.55 kW, scan speed ranging from 0.5 to 2 m/min (with a 1 mm beam diameter) in Ar atmosphere. From the detailed investigation, the following conclusions may be drawn:

a. The depth of hardening was found to be proportional to applied power and decreased with increasing in scan speed.

b. The microstructure obtained was dependent on the laser parameters. An optimum choice of laser parameters is essential to avoid incomplete dissolution of carbide, melting of the surface and formation of a hardened layer containing martensite.

c. The microhardness of the surface was increased and varied with the laser parameters. The maximum microhardness was attained (750 VHN) if an optimum choice of parameters was made.

d. The abrasive wear resistance against hardened steel disk shows significant improvement and was directly proportional to the microhardness of the surface. The improvement was due to the presence of martensite and refinement of the microstructure.

e. The optimum processing conditions for the laser surface hardening of medium carbon steel are: at a laser power of 0.95 kW, scan speed = 1 – 1.5 m/min; at a laser power of 1.2 kW, scan speed = 1 – 2.0 m/min; at a laser power of 1.55 kW, scan speed = 1.5 – 2.0 m/min, respectively.

Acknowledgements

A major part of the work was carried out under the FAST TRACK PROJECT SCHEME, DST (SR/FTP/ET-70/2000), New Delhi. Partial financial support from the ISIRD (IIT, Kharagpur), CSIR (22(0356)/02/EMR-II), N. Delhi, BRNS (LPTD/LMG/BRNS/03-04/76/16-1), Bombay and from the DST (SP/S2/K-17/98), New Delhi are gratefully acknowledged.

REFERENCES

[1] K. G. Budinksi (1988). *Surface Engineering for Wear Resistance*, p. 1, Prentice Hall, New Jersey.

[2] K. Sridhar and A. S. Khanna (1998). In: N. B. Dahotre (Ed.), Lasers in Surface Engineering, p. 69. ASM International, Materials Park, Ohio.

[3] A. A. Ablaeev, E. M. Birger, V. V. Divinskic, S. G. Dromodov and L. A. Madvedovskaya (1989). *Met. Sci. Heat Treat*., **31**, 12.

[4] V. V. Divinskii, L. A. Madvedovskaya, G. A. Rainin and V. Svir (1988). *Sov. Electr. Eng*., **59**, 42.

[5] Guang-Xi Lu and Hong Zhang (1990). *Wear*, **38**, 1.

[6] B. L. Mordike, Materials Science and Technology, (eds. R. W. Cahn, P. Haasen, E. J. Kramer), vol.15, VCH, Weinheim (1993), p. 111.

[7] L. E. Rehn, S. T. Picraux and H. Wiedersich (1987). In: L. E. Rehn, S. T. Picraux and H. Wiedersich (Eds.), *Surface Alloying by Ion, Electron and Laser Beam*, p. 1. ASM, Metals Park, Ohio.

[8] W. M. Steen (1991). *Laser Material Processing*, p. 153, Springer Verlag, London.

[9] T. Mura (1982). *Micromechanics of Defects in Solids*, Martinus Nijhoff Publishers, The - Hague, Netherlands.

[10] A. B. Vannes, R. Fougeres and M. Theolier (1974). *Trait. Therm*, **87**, 67.

[11] V. Raghavan (1985). *Physical Metallurgy – Principles and Practice*, p. 51, Prentice Hall of Private Limited, New Delhi